CRYSTAL GROWTH & DESIGN

Article

Cite This: Cryst. Growth Des. 2019, 19, 2927−2935

pubs.acs.org/crystal

Structure−Function of MamC Loop and Its Effect on the in Vitro Precipitation of Biomimetic Magnetite Nanoparticles

Ana Ubago-Rodríguez,[†,‡,#] Salvador Casares Atienza,[‡,#] Antonia Fernández-Vivas,[†] Ana Peigneux,[†] Ylenia Jabalera,[†] Mario de la Cuesta-Rivero,[†] Concepción Jimenez-Lopez,[*,†] and Ana I. Azuaga Fortes[*,‡]

[†]Department of Microbiology and [‡]Department of Physical Chemistry, University of Granada, Campus de Fuentenueva s/n, 18071, Granada, Spain

ABSTRACT: MamC, an integral protein of the magnetosome membrane, has recently been proposed as a strong candidate to produce biomimetic (magnetosome-like) magnetite nanoparticles that could be used as an alternative to magnetosomes in different applications such as nanocarriers. The secondary structure of the protein contains two helical transmembrane domains connected by an α-helical loop oriented toward the magnetosome lumen. In this loop, the residues Glu66 and Asp70 seem to be responsible for a template effect that controls the nucleation and/or growth of biomimetic nanoparticles in vitro. In the present study, we have introduced a double mutation, E66A and D70A, in the sequence of MamC while working, for the first time, with the full-length protein. Our results show that this double mutation does not affect either the conformation or the stability of MamC, but it indeed makes the protein lose its functionality in terms of controlling the process of magnetite biomineralization in vitro. The present study shows that the ionotropic effect is not enough to account for the effect of the wild type MamC on the formation of BMNPs, but the template effect seems to rule such a process. Also, it shows that no other region of MamC is involved in controlling the process of magnetite biomineralization. Moreover, the stability of MamC in solution is only marginal, probably due to the absence of contacts established with the membrane lipid bilayer.

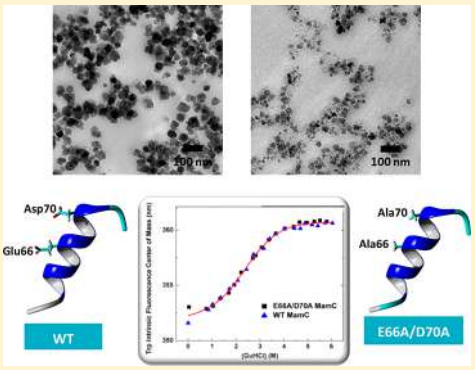

INTRODUCTION

The in vitro production of biomimetic magnetite nanoparticles (BMNPs) with novel magnetic properties by the mediation of magnetosome-associated proteins (MAPs) requires a better understanding on how those MAPs affect the kinetics of magnetite nucleation and growth. Among these MAPs, MamC has recently gained attention because large and well crystallized BMNPs could be obtained by introducing this protein in the solution from which magnetite precipitates.[1] These BMNPs are super-paramagnetic at room temperature and present a large magnetic moment per particle and relatively high magnetization saturation under the influence of a magnetic field.[2] Moreover, MamC attaches to the BMNPs conferring them novel surface properties with functional groups that allow functionalization/release of molecules based on electrostatic interactions and sensitivity to the environmental pH, making these BMNPs strong candidates for a targeted chemotherapy.[2] Therefore, getting a deeper understanding on how MamC controls the formation of BMNPs is crucial to design novel and optimized magnetic nanoparticles.

As any protein with domains rich in acidic amino acids, MamC is able to bind Fe cations due to an ionotropic effect.[1,3−6] However, MamC shows a unique feature in comparison to other MAPs: it can also provide a template for magnetite nucleation, as the distance between Glu66 and Asp70 in the MamC loop matches that between Fe cations in magnetite structure.[4] In fact, when the structure of the MamC loop[5] is compromised or any of these amino acids is not present,[3,4] the magnetite crystals obtained are similar in size than those produced in the absence of the protein. This template effect then seems to be crucial to modify the kinetics of the in vitro nucleation as well as the growth of magnetic nanoparticles. However, the only studies done so far to determine the role of MamC loop on the in vitro magnetite precipitation are based on a chimeric fusion construct of the maltose binding protein and peptides that contain the amino acid sequence of the MamC loop (MBP−MamC−MIP).[4,5]

Proteins are generally seen nowadays as complex statistical ensembles of multiple conformational states.[7−9] Indeed, distal point mutations in a protein can affect the original affinity of binding sites for their ligands as well as their conformational stability in a so-called long-range functional cooperativity and allosteric regulation states. Therefore, the local effect associated with a single point mutation in a protein can be effectively transmitted through an intricate network of cooperative interactions to other regions of the protein, even

Received: January 30, 2019
Revised: March 11, 2019
Published: March 27, 2019

DOI: 10.1021/acs.cgd.9b00150
Cryst. Growth Des. 2019, 19, 2927−2935

far away from the mutation point, and interestingly, these long-range interactions can play a key role in the overall stability of protein molecules.[7−9] Therefore, whether or not the results extracted from the chimera MBP−MamC−MIP study could be extrapolated to the full-length protein, as well as the detailed role of this protein on magnetite formation in vitro and in vivo, remains unknown.

The present study employs the full-length protein to investigate whether or not a double mutation E66/D70 (here referred to as E66A/D70A MamC) could affect not only its leading functional role in the biomineralization process but also the conformational stability of the full-length protein MamC. Hence, the conformation of this double mutant has been analyzed and compared to that of the MamC wild type (here referred to as WT MamC), and the BMNPs resulting by the mediation of both proteins have also been investigated.

EXPERIMENTAL SECTION

Protein Cloning, Expression, and Purification. The mutant E66A/D70A was engineered by introducing a double mutation in the codons corresponding to amino acids Glu66 and Asp70 of the MamC gene, located in the loop of the protein (ProteoGenix, France), and was cloned into the pTrcHis-TOPO vector (Invitrogen, Spain). The competent *Escherichia coli* Rosetta (DE3) strain was transformed with the plasmid described above and grown in LB broth supplemented with ampicillin (50 mg/mL). The culture was incubated at 37 °C with shaking until an optical density of 0.7 (λ = 600 nm) was reached. At that time, protein expression was induced by adding 1 mM IPTG to the culture, and it was overexpressed at 37 °C for 5 h. The cell pellet was collected by centrifugation for 10 min at 6000x*g* and 4 °C and was finally resuspended in lysis buffer (20 mM NaPi pH 7.8, 500 mM NaCl, 1 mM MgCl, 1 mg/mL DNaseI, and protease inhibitors cocktail). Resuspended cells were frozen at −80 °C until use.

Cells were thawed and lysed using a French press. The crude lysate was then ultracentrifuged for 30 min at 104000x*g* and 4 °C. The supernatant was loaded onto a His-Trap Chelating HP (GE Healthcare) following the protocol described by Valverde-Tercedor et al.[1] Finally, the resulting protein sample was loaded onto a size-exclusion column (HiLoad Superdex 200, GE Healthcare Life Sciences) as a polishing step.

Fractions containing MamC protein were refolded by dialyzing against 1 L of buffer A (50 mM Tris, 150 mM NaCl, 6 M urea, pH 8.5) and diluted stepwise 1:2 (twice) with buffer B (50 mM Tris, 150 mM NaCl, pH 8.5) every 3−4 h. Finally, it was dialyzed against buffer B overnight. The purity of the isolated protein was checked by SDS-PAGE and stored at −80 °C until analysis. Both E66A/D70A MamC and WT MamC were stored in the same buffer and equally concentrated prior to use in biomineralization experiments.

Biophysical Characterization of E66A/D70A MamC Protein. Conformational stability of the protein was studied by using standard physical chemistry techniques: circular dichroism (CD) and fluorescence by investigating the secondary structure and the tertiary structure, respectively. CD analyses were carried out using a JASCO J-715 spectrometer (JASCO, Japan) at 25 °C in the far-UV region (210−260 nm) with a 1 nm bandwidth and a scan rate of 100 nm/min. Five scans of each sample were accumulated and the background spectrum (buffer B) was subtracted. To obtain the denaturation curve, a chaotropic agent (guanidinium hydrochloride, Gdn·HCl) was used at increasing concentrations ranging from 0 to 6 M. Subsequently, the sample protein concentration was determined spectrophotometrically, and the actual concentration of Gdn·HCl was checked by measuring the refractive index of the different protein samples prepared with a manual refractometer (ATAGO, Japan).

Fluorescence analyses were performed with a CARY Eclipse fluorescence spectrophotometer (Agilent Technologies, Santa Clara, CA, USA) equipped with a Peltier-controlled thermostatized cell holder. Excitation wavelength was set to 280 nm, and emission spectra were recorded from 300 to 460 nm, at 25 °C, using 5 nm slits and averaging for five scans. The same samples used for the above-mentioned CD study were used here. Changes in protein tertiary structure upon increasing the concentration of Gdn·HCl were estimated via the spectral center of mass (CM). This CM is calculated with the following equation:

$$\mathrm{CM} = \frac{\sum F_i \mathrm{wl}_i}{\mathrm{wl}_i}$$

where F_i is the fluorescence signal at a given wavelength and wl_i is the wavelength.

In addition, dynamic light scattering (DLS) was used to monitor protein size in a DynaPro MSX instrument (Wyatt, Santa Barbara, CA, USA) using a thermostatized 30 μL quartz cuvette. The protein solution and the buffer were centrifuged and filtered through 0.02 μm Anotop filters (Whatman plc, Brentford, Middlesex, UK) before the measurements. Temperature was set to 25 °C, and DLS data were acquired every 10 s until saturation of the signal. Dynamics v.6 software was used in data collection and processing to finally obtain the particle size distributions.

Biomineralization Experiments. Synthesis and materials handling were carried out inside a Coy anaerobic chamber to avoid the potential oxidation of the product, which was filled with 4% H_2 under an N_2 atmosphere, and maintained at room temperature and 1 atm total pressure.

All reagents used in the biomineralization experiments were purchased from Sigma-Adrich (Merck, Darmstadt, Germany). Deoxygenated solutions of $FeCl_3$ (1 M), $Fe(ClO_4)_2$ (0.5 M), $NaHCO_3/Na_2CO_3$ (0.15 M/0.15 M), and NaOH (5 M) were prepared by using deoxygenated Milli-Q water purification. The deoxygenation of the water was carried out by boiling nanopurified water for 1 h and then cooling in an ice bath while continuously bubbling with ultrapure N_2.

Different volumes of the solutions listed in the previous paragraph were mixed to prepare the precipitation solution for the inorganic control experiments (protein-free) to a final composition of $FeCl_3$ (5.56 mM), $Fe(ClO_4)_2$ (2.78 mM), $NaHCO_3/Na_2CO_3$ (3.5 mM/3.5 mM), and pH 9. Identically, BMNPs were precipitated by adding to the mixture above a volume of the purified protein to reach a final concentration of 10 μg/mL. All experiments were run from the same batch of master solution referred to above, and three replicates were prepared for each experiment. When the experiments were repeated, the three series of experiments were always run in parallel: inorganic control experiment, E66A/D70A MamC, and WT MamC to rule out the potential effect on the results of slight experimental changes. Results from each replicate were always similar, with small (not significant) variations in the size histograms. Also, the average sizes of the nanoparticles from each one of the replicates always fell within one standard deviation, the differences in size being not significant for a given set of samples. Each reaction was allowed to proceed inside the anaerobic chamber for 30 days, after which the precipitated materials were harvested. The precipitated solids were concentrated in tubes with a magnet, while the supernatants, which were transparent and contained no visible solids, were discarded. The precipitates were washed with deoxygenated water. This washing procedure was repeated three times, after which the precipitate was collected, immediately freeze-dried, and stored inside the Coy chamber until their analysis.

Characterization of the Solids. Powder samples of the precipitates were analyzed with an Xpert Pro X-ray diffractometer (PANalytical; The Netherlands) using the Cu Kα radiation, with the scan range set from 20 to 60° in 2θ (0.01°/step; 3 s per step). Identification of the precipitates was performed by using the XPowder software. The morphology and size of the magnetite nanoparticles collected in those experiments were studied by transmission electron microscopy (TEM) using a LIBRA 120 PLUS of Carl Zeiss SMT microcope. Magnetic nanoparticles were embedded in Embed 812 resin. Ultrathin sections (50−70 nm) were prepared using a Reichert Ultracut S microtome (Leica Microsystems GmbH, Wetzlar, Germany) after which the sections were deposited onto copper

DOI: 10.1021/acs.cgd.9b00150
Cryst. Growth Des. 2019, 19, 2927−2935

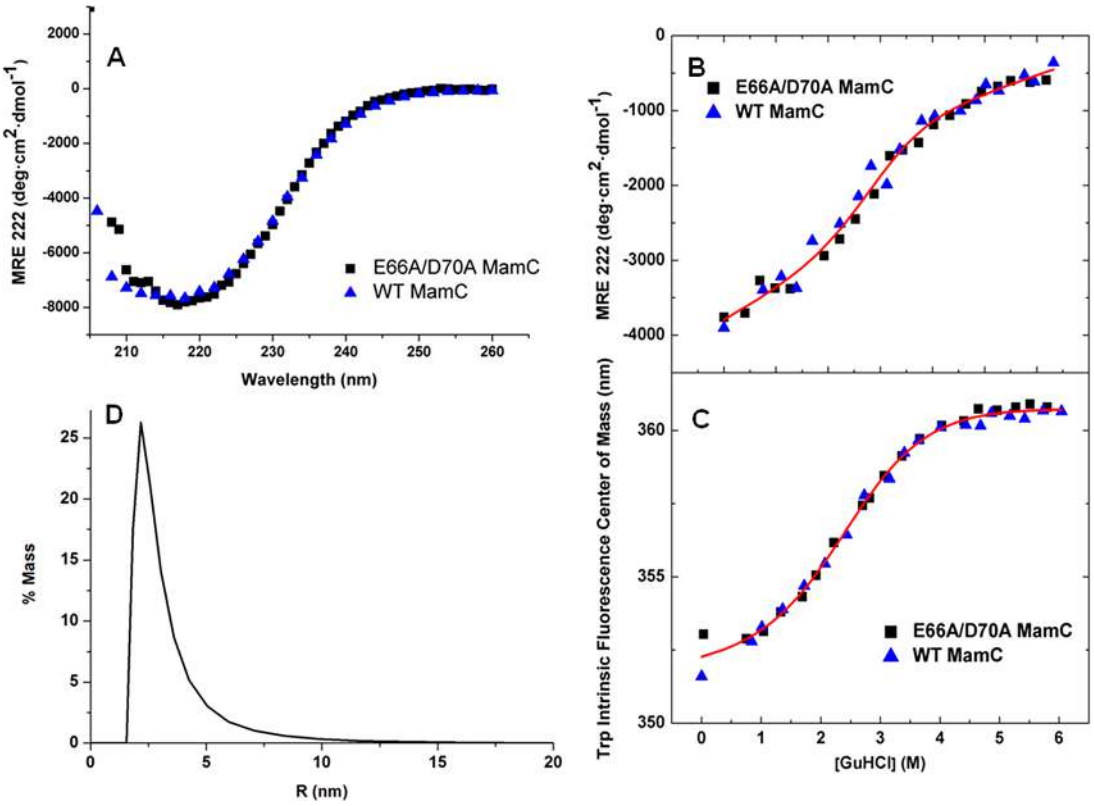

Figure 1. (A) CD spectra of both variants (WT and E66A/D70A mutant) in the far-UV region showing identical secondary structure content. The data have been normalized to molar ellipticity. (B, C) Gdn·HCl chemical denaturation of the two MamC variants studied: WT and E66A/D70A mutant, at 25 °C and pH 8.5, followed by (B) far-UV CD at 222 nm and (C) Trp intrinsic fluorescence. The red line corresponds to a two-state model fit to both data sets simultaneously. (D) Dynamic light scattering results showing the size and the percentage of E66A/D70A MamC protein particles.

grids. The determination of the size of the crystals was done on TEM images taken at 20 kX magnification. To ensure reproducibility of results, crystal sizes were measured on several micrographs at 20 KX with an excess of 1000 nanoparticles for each experiment. The size distribution curves were determined from those measurements by using Origin pro 9. In addition, statistical significance of the results obtained was tested using the Tukey test with a fixed value of $\alpha < 0.05$.

In Silico Mutational Analysis of MamC Functional Loop. Changes in stability of MamC upon mutations were tested using FoldX empirical force field.[10] Since no high-resolution structure of *Magnetococcus marinus* MamC is available to date, a 2.8 Å resolution crystallographic structure of a chimeric construct of the MamC-active loop of *Magnetospirillum magneticum* AMB-1 (MBP-MamC-MIP),[4] PDB code 5e7u, was used instead. Mutations were done on residues E373 and D377 of the MBP−MamC−MIP construct, which correspond to E66 and D70 residues of the full-length *M. marinus* MamC protein.

Default parameters (pH 7, 25 °C and 0.05 M ionic strength) were set for one single run of the force field to mutagenesis completion. Alternatively, as a double check, changes in MamC stability upon mutations were also examined utilizing a support vector machine (SVM)-based computational tool, i-Mutant 2.0,[11] which is purely based on protein amino acid sequence considerations, and setting again pH and temperature at default values, 7 and 25 °C respectively. A full-length *M. marinus* WT MamC amino acid sequence was used in this case.

In addition, we also evaluated the effects of these two mutations on the MamC-active loop conformation. The WT MBP−MamC−MIP chimeric construct and the double mutant (E66A/D70A) were structurally superimposed using a multiple alignment algorithm, MUSTANG,[12] using again default parameters.

RESULTS

Characterization of Wild Type MamC and E66A/D70A Mutant. Circular dichroism (CD) spectra of each sample show that both MamC and the E66A/D70A MamC mutant fold identically, regardless of the presence of the mutation in the protein. In both cases the spectra are characterized by the presence of a minimum at 222 nm (Figure 1A) characteristic of an α-helical conformation, which is consistent with the MamC theoretical structure presented by Nudelman et al.[13]

The unfolding of both proteins upon increasing concentration of denaturant was followed by CD (secondary structure) and fluorescence emission (tertiary structure). In both cases the unfolding of the protein is cooperative as indicated by the presence of a sigmoidal signal and the concomitant loss of secondary and tertiary structure (Figure 1B,C). The unfolding data of both proteins can be fitted to a single two-state denaturation model. The global fitting of the CD and fluorescence data for both proteins yield average values of 2.5 ± 0.2 kJ mol^{-1} M^{-1} for $m_{1/2}$ and ∼11 ± 1 kJ K^{-1} mol^{-1} for the free energy of unfolding for both proteins, regardless of the technique considered. The association state of the proteins (WT MamC and E66A/D70A MamC) was analyzed by dynamic light scattering. At zero concentration of Gnd·HCl, both samples show a main peak (∼90% of the protein) with a molecular size of 2.9 ± 1.0 nm that corresponds to a MamC monomer[3] (Figure 1D).

In Silico Mutagenesis Study. In silico mutagenesis of the MamC-active loop in residues E66 and D70 for alanine was accomplished using a FoldX force field.[10] There is no high-

DOI: 10.1021/acs.cgd.9b00150
Cryst. Growth Des. 2019, 19, 2927−2935

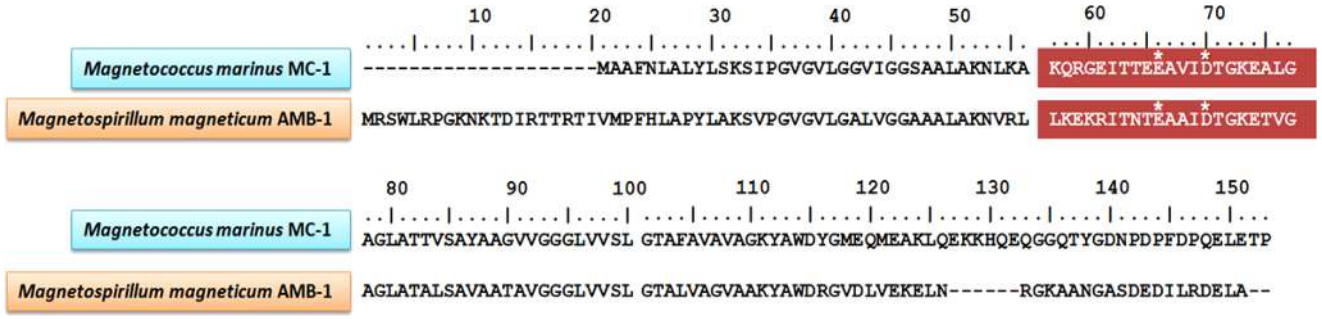

Figure 2. Sequences alignment of MamC protein from *M. marinus* strain MC-1 and *Ms. magneticum* strain AMB-1. Amino acids of the proteins' loop are red shaded, and the two mutated amino acids (Glu66 and Asp7) are indicated with white stars. According to the BLAST analysis, we obtained that both sequences have a homology percentage of 69%.

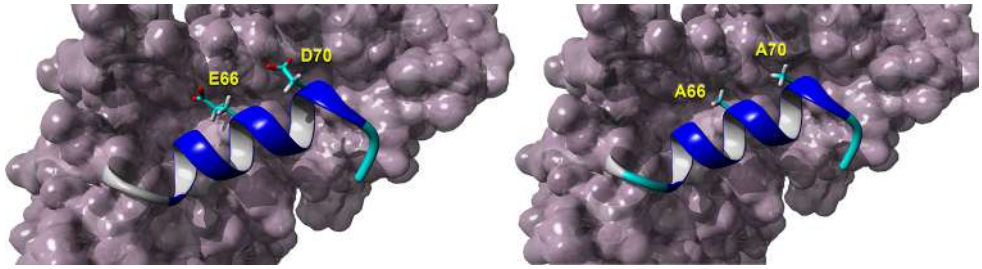

Figure 3. 3D model structure of the MBP−MamC−MIP chimeric fusion protein (5e7u PDB code). (A) Wild type MamC loop construct and (B) E66A/D70A double mutant. van der Waals surface of the fusion protein is represented in light magenta, and the MamC loop is represented in ribbon. Residues 66 and 70 are shown in sticks.

resolution structure of *M. marinus* full-length MamC available to date, and the MBP−MamC−MIP chimeric construct is the closest model we could use as a template for this study, considering the high sequence homology that the MamC protein active loop of these two microorganisms share (Figure 2). On the other hand, a different computer-based protein stability prediction tool, i-Mutant 2.0,[11] was used (considering the same parameters previously set for FoldX force field) to test for the effect of these two mutations on *M. marinus* MamC. As opposed to FoldX, the i-Mutant algorithm is able to estimate changes in stability of proteins based on the amino acid sequence. Both computational tools yielded a nearly identical $\Delta\Delta G_{mut}$ value less than 4 kJ·mol^{-1}, which indicates that the overall energetics of the protein is not affected by this double mutation.

In addition, the MBP−MamC−MIP chimeric fusion construct and the mutated variant E66A/D70A-MBP−MamC−MIP were structurally superimposed using MUSTANG[12] to check for potential structural rearrangements within the MamC loop around the mutation points. Several rounds of iteration were completed to allow the algorithm convergence to a final value of RMSD of 0.000 over the 380 residues of both full-length constructs aligned. This RMSD value implies that both structures are nearly identical, and therefore these two mutations do not affect the MamC-active loop conformation (Figure 3).

Characterization of Solids. The solids formed in all biomineralization experiments were identified as being 100% magnetite using XRD. TEM analysis of the magnetite particles produced in the inorganic (protein-free) control (Figures 4A−B) and the E66A/D70A MamC experiments (Figure 4C−D) show an average of crystal sizes of 16 ± 6 nm and 17 ± 4 nm, respectively, this difference being not statistically significant (Figure 5). The shift of the size distribution curve to lower sizes in the case of E66A/D70A MamC nanoparticles is due to the presence of Tris buffer whose inhibitory effect on magnetite nucleation has already pointed out by Kuwahara et al.[14] and Lopez-Moreno et al.[3] Different is the case of the magnetite crystals obtained in the presence of wild type MamC (Figure 4E−G). At 10 μg/mL of MamC, magnetite crystals displayed well-developed crystal faces and sizes of 36 ± 11 nm. Our analyses show that this size difference is statistically significant in comparison to that of the magnetite nanoparticles obtained in the inorganic control or in the presence of E66A/D70A MamC.

DISCUSSION

MamC is a small integral membrane protein (12.4 kDa) with two transmembrane helices connected by a small peptide (~21 amino acids) directed into the magnetosome lumen. The use of this protein to form biomimetic nanoparticles implies to include MamC into water-based solutions, and it is in this environment in which MamC needs to maintain its functionality, which previous studies linked to its conformation.[3−5] Magnetosome membrane associated proteins are among the few integral membrane proteins that are water-soluble.[15] Indeed, as the secondary structure of MamC both in the presence and in the absence of detergent is the same,[3] it can be inferred that detergents do not affect the conformation of the protein, and, therefore, detergents are not necessary for MamC to reach its active conformation. As previously shown by Lopez-Moreno et al.[3] MamC in aqueous solution exists as an equilibrium mainly populated by dimeric and trimeric species. This water-soluble assembly could prevent the aggregation of MamC in the absence of detergent by sequestering hydrophobic patches from water.

The knowledge of the forces stabilizing soluble proteins basically relies on thermodynamic studies of the folding/

DOI: 10.1021/acs.cgd.9b00150
Cryst. Growth Des. 2019, 19, 2927−2935

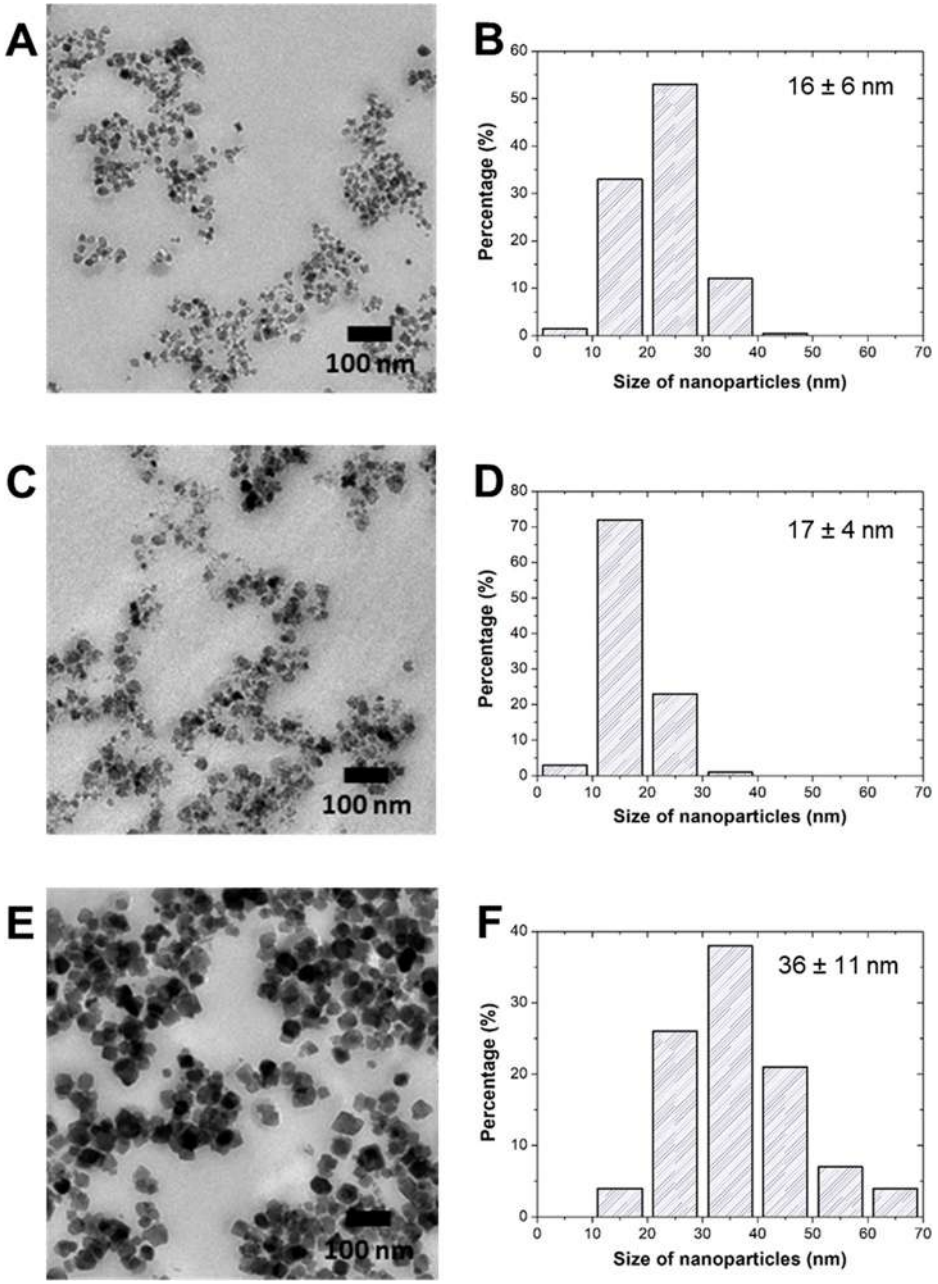

Figure 4. TEM images of magnetite nanoparticles obtained in different experimental conditions. (A and B) Magnetite crystals from the inorganic control experiment and size distribution; (C and D) magnetite crystals from the E66A/D70A MamC experiment and size distribution; (E and F) Magnetite crystals from the WT MamC experiment and size distribution.

unfolding process[16] induced by heat[17] or chemical denaturants.[18] Yet this approach has not been widely applied to membrane proteins due to the resistance that they show to undergo a complete denaturation for being part of the membrane suprastructure themselves. In other words, the intimate interaction these proteins establish with the membrane lipidic bilayer protects the protein structure from completely unfolding. However, in recent years several reversible unfolding studies have been attained for a few membrane proteins, such as bacteriorhodopsin,[19,20] diacylglycerol kinase,[21] the KcsA potassium channel,[22] disulfide bond reducing protein DsbB,[23] *Archaeoglobus fulgidus* CopA,[24] rhomboid intramembrane proteases,[25] and some outer membrane proteins.[26−30] However, being MamC soluble in aqueous solution, a conventional chemical denaturation monitored by circular dichroism and Trp intrinsic fluorescence spectroscopy could be applied for both the wild type (WT) and the double mutant E66A/D70A MamC. MamC becomes, therefore, one of the few examples of membrane proteins studied so far and, out of them, one of the very few where no detergents or lipid micelles were necessary to keep it soluble in aqueous solution.

The unfolding by chemical denaturation of both protein variants followed by CD and fluorescence is fully cooperative, with a sigmoidal-shaped transition compatible with a two-state mechanism; i.e., only two species are significantly populated throughout the unfolding process the native and the unfolded states. The loss of secondary and tertiary structures occurs concomitantly, with a $m_{1/2}$ value around 2.5, which also indicates a cooperative unfolding of the protein, i.e., in one

DOI: 10.1021/acs.cgd.9b00150
Cryst. Growth Des. 2019, 19, 2927−2935

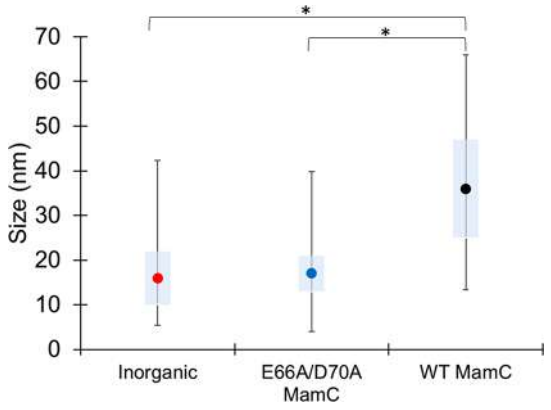

Figure 5. Box plot of the size of magnetite nanoparticles obtained in inorganic, E66A/D70A MamC experiments and WT MamC experiments. Statistical differences among all samples were calculated using Student's T-test, taking $T > 1.65$ as a critical value to indicate statistical significance. Asterisks mean statistical significance, while the lack of an asterisk means no statistical significance.

single step (no significantly populated folding intermediates detected). In addition, both WT MamC and E66A/D70A MamC seem to be in a monomeric state in solution at the concentration conditions used in these experiments, as inferred from a hydrodynamic radius of 2.9 ± 1.0 nm, which corresponds to a monomer for a protein size like MamC's.[3]

In summary, the low concentration of MamC used allows the protein to remain soluble and monomeric in water solution, and a simple two-state model can be used to fit the chemical unfolding data. The global fitting of all unfolding transitions to a two-state model gives very low free energy of unfolding and $m_{1/2}$ values in comparison to those obtained for globular proteins of similar size, which usually range between 20−80 kJ·mol^{-1} and 5 respectively. Similar values are observed with other integral membrane proteins.[23,31] This marginal stability of the protein in aqueous solution is probably overcome with the insertion of MamC within the membrane and/or with its self-oligomerization, which would stabilize the conformation of the protein as detailed below. The stability of MamC like other folded membrane proteins resides in a free energy minimum determined by the net energetics of the interactions of the peptide chains with water, to each other, to the lipid bilayer and cofactors.[22,32] Therefore, such a marginal stability observed for MamC in aqueous solution is not surprising.

In terms of the role of MamC on the in vitro formation of BMNPs, as demonstrated by Bereczk-Tompa et al.,[33] many surfaces could serve as sites for magnetite nucleation, especially if electrostatic interactions between negatively charged amino acids of proteins and Fe cations come into play through an ionotropic effect, meaning a local increase in the supersaturation of the system with respect to magnetite caused by the concentration of the Fe cations in the acidic regions of the proteins.[1,3−5] These authors also demonstrated that iron binding by negatively charged amino acids is a less specific process than the binding of previously formed nuclei, suggesting that the magnetite nucleation under their conditions occurred by charge accumulation (ionotropic effect). It was previously shown that MamC is able to bind Fe cations,[1] and it is also able to bind to magnetite,[4] so both nucleation mechanisms could occur in our system. Along these lines, a recent study[6] also shows the interaction of MamC via the Asp 70 amino acid located in the MamC loop, with Fe cations. According to the results of Bereczk-Tompa et al.[33] and the former being less selective, magnetite nucleation induced by the ionotropic effect is probably kinetically favored. HRTEM images of MamC-mediated magnetite crystals in Lopez-Moreno et al.[3] showing that they are single crystals with no discontinuities in the crystal lattices also support this hypothesis versus the oriented aggregation of previously formed nuclei.

In this context, it seems clear that heterogeneous protein-mediated nucleation would lead to the formation of less nuclei compared to an homogeneous nucleation occurring in the bulk solution. In fact, in the protein-free experiments, and since the system is supersaturated with respect to magnetite [$\log\Omega_{magnetite} = 22.57$][1] bulk nucleation occurs, giving rise to the formation of a large number of crystals with a small size, probably the restricted concentration of Fe cations being the limiting step for crystal growth. On the contrary, both E66A/D70A MamC and WT MamC provide negatively charged amino acids that would act as nucleation sites thanks to the ionotropic effect, thus kinetically favoring magnetite nucleation at those sites versus bulk nucleation. Indeed, MamC from MC-1 contains five amino acids negatively charged that represent 15.6% of the total amino acids of the loop. However, this may not be the only effect accounting for magnetite nucleation. On one hand, if the ionotropic effect was the only one to be claimed on magnetite nucleation, still some effect on the magnetite nucleation and/or growth processes resulting in different crystals compared to the inorganic control would be expected in the E66A/D70A MamC bearing experiments. But crystals from experiments containing E66A/D70A MamC do not show any significant difference in comparison to those from the inorganic control, also indicating that no other region of the protein is involved in controlling the process of magnetite biomineralization. On the other hand, out of the five acidic amino acids in the WT MamC loop, two of them were replaced by alanine (nonpolar) in E66A/D70A MamC. Therefore, if the ionotropic effect was the only one accounting for magnetite nucleation, fewer nucleation sites would be provided by E66A/D70A MamC compared to those provided by WT MamC, and, therefore, fewer and larger crystals would be expected in the presence of the former (E66A/D70A MamC). However, we found the opposite effect. Thus, in this case, the change in the number of charges cannot explain the change observed in magnetite nucleation. Thus, the ionotropic effect is not the only process involved in magnetite nucleation, and other more specific mechanisms need to be invoked.

Previous studies[3−5,34] have demonstrated the importance that the right conformation of MamC has on magnetite precipitation in terms of obtaining large crystals. If this conformation is altered somehow, then those large crystals do not form. Specifically, Nudelman and co-workers have shown that two specific amino acids located at the MamC loop, Glu66 and Asp70, are responsible of the template effect that controls magnetite nucleation and growth in vitro, which, in turn results in larger and better faceted magnetite nanoparticles.[5] Yet these authors utilized a chimeric fusion construct of the maltose binding protein (MBP) and the active loop of MamC of *Ms. magneticum* in different positions within the MBP.[4,5] According to these authors, the spacing between Glu66 and Asp70 (8 Å) is the responsible for the surface matching that is similar (within the helix elasticity) to the 6 Å distance between the Fe cations in specific crystal faces, namely, (111), (100), (110),

DOI: 10.1021/acs.cgd.9b00150
Cryst. Growth Des. 2019, 19, 2927−2935

and (311). Those faces precisely become expressed in the WT MamC-mediated magnetite crystals and not in those resulting from the inorganic (protein-free) experiments.[3] Indeed, as the results from the present manuscript demonstrate, the orientation of the side chains of these two amino acids within the alpha helical structure of the loop is essential for MamC, providing a template for magnetite growth, as shown by the lack of functionality of the double mutant E66A/D70A MamC. The novelty of the present work lies in the fact that this effect is demonstrated not in a chimera, but using the full-length protein MamC.

These observations therefore suggest the existence of a template effect that would be the most kinetically favored process for magnetite nucleation, thus initiating the formation of magnetite nuclei at those precise sites and lowering the number of nuclei compared to any other condition (inorganic experiment or E66A/D70A MamC). Once formed, these nuclei grow, first probably at the expenses of the Fe available in the bulk solution, and later, from the Fe previously bound by the acidic amino acids in other regions of the protein (including the other acidic amino acids in MamC loop), which then act as Fe reservoirs for crystal growth. Hence, crystal growth would continue until the system becomes subsaturated with respect to magnetite. In this scenario, MamC-mediated magnetite precipitation produces the largest crystals compared to those obtained in the rest of the experiments.

As mentioned earlier, despite the effect that this double mutation causes in MamC biomineralization activity, mutations might also affect protein conformation. Generally speaking, mutations can alter protein conformation from a simple local remodeling to a global structure collapse, when they occur at the main folding core of the protein. However, the latter is not the case of E66A/D70A mutations for MamC, as inferred from the CD and fluorescence results. Replacement of these two amino acids in the active loop of the protein does not affect the overall conformation of MamC apparently. Our CD data support the idea that both the WT MamC and E66A/D70A MamC display nearly identical secondary structure content (Figure 1A). Moreover, Nudelman and co-workers confirmed by X-ray crystallography that the concurrent mutation of residues Glu66 and Asp70 to alanines in *Ms. magneticum* MamC-active loop does not affect the alpha helical fold of the loop itself.[4] Since sequence homology of the active loop of both proteins (Figure 4) is quite high, 69% similar behavior of *M. marinus* MamC can be expected, with no structural alteration of its active loop either. Indeed, the structural alignment algorithm MUSTANG[12] predicts a perfect structural superimposition of the two protein variants, WT MamC and E66A/D70A MamC, with a negligible RMSD value, again suggesting that there is no conformational change in the MamC-active loop upon E66A/D70A double mutation.

Moreover, all chemical denaturation curves of the two *M. marinus* MamC variants tested, WT MamC and E66A/D70A MamC, overlap. Therefore, the data collected for them both, either monitoring the secondary or the tertiary structure loss, could be fitted globally to a two-state unfolding model. This clearly supports the idea that this double mutation E66A/D70A does not affect the conformation of the loop or the overall protein structure. These two residues, Glu66 and Asp70, are water exposed in the protein structure, and they are not participating in interactions of any kind (salt-bridges, van der Waals clashes, etc.) with any other residue of the protein. Hence, replacing the side chain of the residues located at these two specific locations of the protein only affects the functional interaction of MamC with the magnetite crystals but has virtually no effect on the conformational stability of the protein.

The in silico mutagenesis analysis derived from FOLDEF, which accounts for changes in protein stability associated with mutations in terms of free energy change ($\Delta\Delta G_{mut}$). In our case, this analysis gave rise to a $\Delta\Delta G_{mut}$ value of less than 4 kJ·mol^{-1} upon this double mutation, something negligible within the overall stability of a protein. These results confirm those we already obtained by the chemical denaturation studies: replacing these two functionally essential residues within the MamC-active loop does not affect it, either structurally or energetically.

Of course, these results could be biased by the fact that this analysis has been carried out by using a fusion construct containing just the functional loop of MamC of a different microorganism attached to MBP, despite the high sequence homology they share. However, as a double check with a different computational tool, i-Mutant 2.0[11] was used to estimate changes in the overall protein energetics upon this double mutation using the exact *M. marinus* MamC protein sequence. This tool is based on a different algorithm not limited to the analysis of a combination of multiple energy terms, but leverages any kind of information available suited to protein stability (local interactions and sequence information). Not surprisingly, i-Mutant 2.0 gave rise to the same $\Delta\Delta G_{mut}$ value that FOLDEF yielded, less than 4 kJ·mol^{-1}, which is indicative that this result is genuine and that there is no change in the MamC-active loop upon the double mutation E66A/D70A (Figure 3).

CONCLUSIONS

In this study, we have confirmed that the crystals formed in the presence of the MamC double mutant E66A/D70A resemble those of inorganic magnetite grown in the absence of protein. Therefore, these two residues are essential for the activity of the protein in terms of providing a template for magnetite growth resulting in larger and better faceted particles. Moreover, this template effect could be claimed as the one that governs magnetite nucleation and/or growth, since the ionotropic effect that could still be exerted by the acidic amino acids in the E66A/D70A MamC loop is not enough to mediate the formation of magnetite crystals different than those from the inorganic (protein-free) control experiment. Also, our results show that no other region of MamC is involved in controlling the process of magnetite biomineralization. However, this double mutation does not affect either the conformation or the stability of the protein as shown by CD in the far UV region or tryptophan intrinsic fluorescence. Therefore, Glu66 and Asp70 are not participating in interactions with any other residue of the protein.

Moreover, also our results indicate that the stability of MamC is only marginal, indeed lower that the average stability of proteins this size. The low stability of this protein in aqueous solution is probably the result of the absence of the membrane lipid bilayer, where multiple interactions are established that stabilize the final active conformation of the protein.

DOI: 10.1021/acs.cgd.9b00150
Cryst. Growth Des. 2019, 19, 2927−2935

AUTHOR INFORMATION

Corresponding Authors

*(C.J.L.) E-mail: cjl@ugr.es; tel.: (+34)958249833.
*(A.I.A.F) E-mail: aiazuaga@ugr.es; tel.: (+34)958249366.

ORCID

Concepción Jimenez-Lopez: 0000-0002-5645-2079
Ana I. Azuaga Fortes: 0000-0002-5736-5831

Author Contributions

#A.U.-R. and S.C.A. contributed equally. The manuscript was written through contributions of all authors. All authors have given approval to the final version of the manuscript. A.I.A.F. and S.C.A. designed the CD, fluorescence, and DLS experiments. The double mutant was designed by A.I.A.F. In silico analysis was done by S.C.A. All these biophysical studies were later discussed by A.I.A.F. and S.C.A. C.J.L. and M.A.F.V. planned biomineralization experiments, the characterization of solids, and discussed the results. A.U.R., Y.J.R., and A.P.N. performed the experiments, initiated by M.C.R., and analyzed the samples.

Funding

This research was funded by the Ministerio de Economía y Competitividad (CGL2013-46612 and CGL2016-76723 projects) and the Fondo Europeo de Desarrollo Regional (FEDER).

Notes

The authors declare no competing financial interest.

ACKNOWLEDGMENTS

Y.J.R. is a recipient of an FPU2016 grant (ref FPU16_04580) from the Ministerio de Educación, Ciencia y Deporte y Competitividad (Spain), and C.J.L. thanks the Unidad Científica de Excelencia UCE-PP2016-05 of the University of Granada. A.U.R. is a recipient of a Youth Development and Employment Contract (FEDER funds). We also thank the CIC personnel of the University of Granada for technical assistance in the TEM. Thanks go to Dr. Myerson and two anonymous reviewers whose comments greatly improved the manuscript.

ABBREVIATIONS

BMNPs	biomimetic magnetite nanoparticles
CD	circular dichroism
CM	mass spectral center
DLS	dynamic light scattering
Gnd·HCl	guanidinum chloride
IMAC	immobilized metal affinity chromatography
MAPs	magnetosome-associated proteins
MBP	maltose binding protein
MPs	membrane proteins
MRE	molar residue ellipticity
MTB	magnetotactic bacteria
SVM	support vector machine
TEM	transmission electron microscopy
Trp	tryptophan
Wl	wavelength
WT	wild type
$\Delta\Delta G_{mut}$	difference of Gibbs energy change due to mutation

REFERENCES

(1) Valverde-Tercedor, C.; Montalban-Lopez, M.; Perez-Gonzalez, T.; Sanchez-Quesada, M. S.; Prozorov, T.; Pineda-Molina, E.; Fernandez-Vivas, M. A.; Rodriguez-Navarro, A. B.; Trubitsyn, D.; Bazylinski, D. A.; Jimenez-Lopez, C. Size Control of in Vitro Synthesized Magnetite Crystals by the MamC Protein of Magnetococcus Marinus Strain MC-1. *Appl. Microbiol. Biotechnol.* **2015**, *99*, 5109−5121.

(2) Garcia Rubia, G.; Peigneux, A.; Jabalera, Y.; Puerma, J.; Oltolina, F.; Elert, K.; Colangelo, D.; Gomez Morales, J.; Prat, M.; Jimenez-Lopez, C. PH-Dependent Adsorption Release of Doxorubicin on MamC-Biomimetic Magnetite Nanoparticles. *Langmuir* **2018**, *34*, 13713−13724.

(3) Lopez-Moreno, R.; Fernández-Vivas, A.; Valverde-Tercedor, C.; Azuaga Fortes, A. I.; Casares Atienza, S.; Rodriguez-Navarro, A. B.; Zarivach, R.; Jimenez-Lopez, C. Magnetite Nanoparticles Biomineralization in the Presence of the Magnetosome Membrane Protein MamC: Effect of Protein Aggregation and Protein Structure on Magnetite Formation. *Cryst. Growth Des.* **2017**, *17*, 1620−1629.

(4) Nudelman, H.; Valverde-Tercedor, C.; Kolusheva, S.; Perez Gonzalez, T.; Widdrat, M.; Grimberg, N.; Levi, H.; Nelkenbaum, O.; Davidov, G.; Faivre, D.; Jimenez-Lopez, C.; Zarivach, R. Structure-Function Studies of the Magnetite-Biomineralizing Magnetosome-Associated Protein MamC. *J. Struct. Biol.* **2016**, *194*, 244−252.

(5) Nudelman, H.; Perez Gonzalez, T.; Kolushiva, S.; Widdrat, M.; Reichel, V.; Peigneux, A.; Davidov, G.; Bitton, R.; Faivre, D.; Jimenez-Lopez, C.; Zarivach, R. The Importance of the Helical Structure of a MamC-Derived Magnetite-Interacting Peptide for Its Function in Magnetite Formation. *Acta Crystallogr. D Struct Biol.* **2018**, *74*, 10−20.

(6) Nudelman, H.; Lee, Y. Z.; Hung, Y. L.; Kolusheva, S.; Upcher, A.; Chen, Y. C.; Chen, J. Y.; Sue, S. C.; Zarivach, R. Understanding the Biomineralization Role of Magnetite-Interacting Components (MICs) from Magnetotactic Bacteria. *Front. Microbiol.* **2018**, *9* (OCT), 1−14.

(7) Casares, S.; Sadqi, M.; Lopez-Mayorga, O.; Martinez, J. C.; Conejero-Lara, F. Structural Cooperativity in the SH3 Domain Studied by Site-Directed Mutagenesis and Amide Hydrogen Exchange. *FEBS Lett.* **2003**, *539*, 125−130.

(8) Hilser, V. J.; Dowdy, D.; Oas, T. G.; Freire, E. The Structural Distribution of Cooperative Interactions in Proteins: Analysis of the Native State Ensemble. *Proc. Natl. Acad. Sci. U. S. A.* **1998**, *95*, 9903−9908.

(9) Pan, H.; Lee, J. C.; Hilser, V. J. Binding Sites in Escherichia Coli Dihydrofolate Reductase Communicate by Modulating the Conformational Ensemble. *Proc. Natl. Acad. Sci. U. S. A.* **2000**, *97*, 12020−12025.

(10) Schymkowitz, J.; Borg, J.; Stricher, F.; Nys, R.; Rousseau, F.; Serrano, L. The FoldX Web Server: An Online Force Field. *Nucleic Acids Res.* **2005**, *33*, W382−8.

(11) Capriotti, E.; Fariselli, P.; Casadio, R. I-Mutant2.0: Predicting Stability Changes upon Mutation from the Protein Sequence or Structure. *Nucleic Acids Res.* **2005**, *33*, W306−10.

(12) Konagurthu, A. S.; Whisstock, J. C.; Stuckey, P. J.; Lesk, A. M. MUSTANG: A Multiple Structural Alignment Algorithm. *Proteins: Struct., Funct., Genet.* **2006**, *64*, 559−574.

(13) Nudelman, H.; Zarivach, R. Structure Prediction of Magnetosome-Associated Proteins. *Front. Microbiol.* **2014**, *5*, 9.

(14) Kuwahara, Y.; Miyazaki, T.; Shirosaki, Y.; Liu, G.; Kawashita, M. Structures of Organic Additives Modified Magnetite Nanoparticles. *Ceram. Int.* **2016**, *42* (5), 6000−6004.

(15) Rawlings, A. E. Membrane Proteins: Always an Insoluble Problem? *Biochem. Soc. Trans.* **2016**, *44*, 790−795.

(16) Richards, F. M. Folded and Unfolded Proteins: An Introduction. In *Protein Folding*; Creighton, T. E., Ed.; W. H. Freeman and Company: USA, 1992; pp 1−58.

(17) Privalov, P. Physical Basis of the Stability of the Folded Conformations of Proteins. In *Protein Folding*; Creighton, T. E., Ed.; W. H. Freeman and Company: USA, 1992.

(18) Pace, C. N. Determination and Analysis of Urea and Guanidine Hydrochloride Denaturation Curves. *Methods Enzymol.* **1986**, *131*, 266−280.

DOI: 10.1021/acs.cgd.9b00150
Cryst. Growth Des. 2019, 19, 2927−2935

(19) Curnow, P.; Booth, P. J. Combined Kinetic and Thermodynamic Analysis of Alpha-Helical Membrane Protein Unfolding. *Proc. Natl. Acad. Sci. U. S. A.* **2007**, *104*, 18970−18975.
(20) Faham, S.; Yang, D.; Bare, E.; Yohannan, S.; Whitelegge, J. P.; Bowie, J. U. Side-Chain Contributions to Membrane Protein Structure and Stability. *J. Mol. Biol.* **2004**, *335*, 297−305.
(21) Lau, F. W.; Bowie, J. U. A Method for Assessing the Stability of a Membrane Protein. *Biochemistry* **1997**, *36*, 5884−5892.
(22) Barrera, F. N.; Renart, M. L.; Molina, M. L.; Poveda, J. A.; Encinar, J. A.; Fernandez, A. M.; Neira, J. L.; Gonzalez-Ros, J. M. Unfolding and Refolding in Vitro of a Tetrameric, Alpha-Helical Membrane Protein: The Prokaryotic Potassium Channel KcsA. *Biochemistry* **2005**, *44*, 14344−14352.
(23) Otzen, D. E. Folding of DsbB in Mixed Micelles: A Kinetic Analysis of the Stability of a Bacterial Membrane Protein. *J. Mol. Biol.* **2003**, *330*, 641−649.
(24) Roman, E. A.; Arguello, J. M.; Gonzalez Flecha, F. L. Reversible Unfolding of a Thermophilic Membrane Protein in Phospholipid/Detergent Mixed Micelles. *J. Mol. Biol.* **2010**, *397*, 550−559.
(25) Panigrahi, R.; Arutyunova, E.; Panwar, P.; Gimpl, K.; Keller, S.; Lemieux, M. J. Reversible Unfolding of Rhomboid Intramembrane Proteases. *Biophys. J.* **2016**, *110*, 1379−1390.
(26) Danoff, E. J.; Fleming, K. G. Novel Kinetic Intermediates Populated along the Folding Pathway of the Transmembrane Beta-Barrel OmpA. *Biochemistry* **2017**, *56*, 47−60.
(27) Hong, H.; Tamm, L. K. Elastic Coupling of Integral Membrane Protein Stability to Lipid Bilayer Forces. *Proc. Natl. Acad. Sci. U. S. A.* **2004**, *101*, 4065−4070.
(28) Huysmans, G. H.; Baldwin, S. A.; Brockwell, D. J.; Radford, S. E. The Transition State for Folding of an Outer Membrane Protein. *Proc. Natl. Acad. Sci. U. S. A.* **2010**, *107*, 4099−4104.
(29) Moon, C. P.; Fleming, K. G. Using Tryptophan Fluorescence to Measure the Stability of Membrane Proteins Folded in Liposomes. *Methods Enzymol.* **2011**, *492*, 189−211.
(30) Pocanschi, C. L.; Popot, J. L.; Kleinschmidt, J. H. Folding and Stability of Outer Membrane Protein A (OmpA) from Escherichia Coli in an Amphipathic Polymer, Amphipol A8−35. *Eur. Biophys. J.* **2013**, *42*, 103−118.
(31) Booth, P. J.; Curnow, P. Folding Scene Investigation: Membrane Proteins. *Curr. Opin. Struct. Biol.* **2009**, *19*, 8−13.
(32) MacKenzie, K. R.; Fleming, K. G. Association Energetics of Membrane Spanning Alpha-Helices. *Curr. Opin. Struct. Biol.* **2008**, *18*, 412−419.
(33) Bereczk-tompa, É.; Vonderviszt, F.; Horváth, B.; Szalai, I.; Pósfai, M. *Nanoscale* **2017**, *9*, 15062−15069.
(34) Jabalera, Y.; Casares Atienza, S.; Fernández-Vivas, A.; Peigneux, A.; Azuaga Fortes, A. I.; Jimenez-Lopez, C. Protein Conservation Method Affects MamC-Mediated Biomineralization of Magnetic Nanoparticles. *Cryst. Growth Des.* **2019**, *19*, 1064.

DOI: 10.1021/acs.cgd.9b00150
Cryst. Growth Des. 2019, 19, 2927−2935